AD-A056 237 ARMY ARMAMENT RESEARCH AND DEVELOPMENT COMMAND DOVER--ETC F/G 9/6
ERROR PROBABILITY IN BINARY DIGITAL FM TRANSMISSION SYSTEMS.(U)
FEB 78 W DONNALLY

UNCLASSIFIED ARTSD-TR-77006 SBIE-AD-E400 090 NL

| OF |
AD
A056237

END
DATE
FILMED
8 -78
DDC

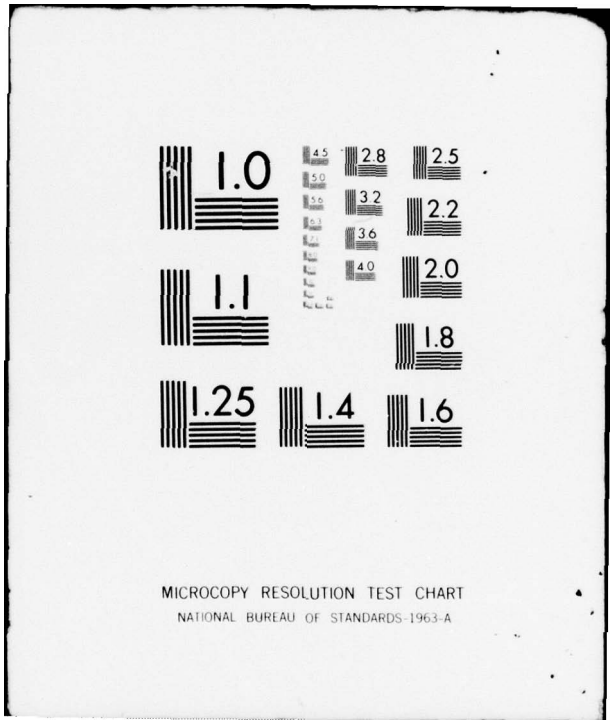
1.0
1.1
1.25
1.4
1.6
1.8
2.0
2.2
2.5
2.8
3.2
3.6
4.0
4.5
5.0
5.6
6.3
MICROCOPY RESOLUTION TEST CHART
NATIONAL BUREAU OF STANDARDS-1963-A

1

(12) LEVEL II

27 Apr 78

AD

AD-E400 090

TECHNICAL REPORT ARTSD-TR-77006

ERROR PROBABILITY IN BINARY DIGITAL FM TRANSMISSION SYSTEMS

WILLIAM DONNALLY

FEBRUARY 1978

US ARMY ARMAMENT RESEARCH AND DEVELOPMENT COMMAND
TECHNICAL SUPPORT DIRECTORATE
DOVER, NEW JERSEY

The findings in this report are not to be construed as an official Department of the Army position.

DISPOSITION

Destroy this report when no longer needed. Do not return to the originator.

UNCLASSIFIED

SECURITY CLASSIFICATION OF THIS PAGE (When Data Entered)

REPORT DOCUMENTATION PAGE

READ INSTRUCTIONS BEFORE COMPLETING FORM

1. REPORT NUMBER: ARTSD-TR-77006	2. GOVT ACCESSION NO.
3. RECIPIENT'S CATALOG NUMBER	
4. TITLE (and Subtitle): ERROR PROBABILITY IN BINARY DIGITAL FM TRANSMISSION SYSTEMS	5. TYPE OF REPORT & PERIOD COVERED: Technical rept.
	6. PERFORMING ORG. REPORT NUMBER
7. AUTHOR(s): William Donnally	8. CONTRACT OR GRANT NUMBER(s): AMCMS 662617H790211
9. PERFORMING ORGANIZATION NAME AND ADDRESS: Commander, Picatinny Arsenal, TSD, Dover, NJ 07801	10. PROGRAM ELEMENT, PROJECT, TASK AREA & WORK UNIT NUMBERS: Feb 78
11. CONTROLLING OFFICE NAME AND ADDRESS: ARRADCOM, TSD, Instrumentation Div (DRDAR-TSI-T), Dover, NJ 07801	12. REPORT DATE: FEBRUARY 1978
	13. NUMBER OF PAGES: 27 (12) 24p.
14. MONITORING AGENCY NAME & ADDRESS (if different from Controlling Office)	15. SECURITY CLASS. (of this report): UNCLASSIFIED
	15a. DECLASSIFICATION/DOWNGRADING SCHEDULE

16. DISTRIBUTION STATEMENT (of this Report)

Approved for public release; distribution unlimited.

17. DISTRIBUTION STATEMENT (of the abstract entered in Block 20, if different from Report)

18. SBIE

19. AD-E400 090

18. SUPPLEMENTARY NOTES

19. KEY WORDS (Continue on reverse side if necessary and identify by block number)

Telemetry	Discriminators	Error rate
Frequency modulation	Modulation	Transmission system
Digital modulation	Angular feedback	Error probability
Communications	Pulse-code modulation	Phase-lock

20. ABSTRACT (Continue on reverse side if necessary and identify by block number)

The information presented in this report concerns the analysis of error probability in various binary, digital, frequency modulated (FM) transmission systems operating in the presence of additive noise. The actual "error producing" mechanism, associated with digital FM modulation techniques, is analyzed. This report will aid the design engineer in determining the advantages and disadvantages associated with each type of modulation and the particular advantages of

next page

DD FORM 1 JAN 73 1473 EDITION OF 1 NOV 65 IS OBSOLETE

UNCLASSIFIED

SECURITY CLASSIFICATION OF THIS PAGE (When Data Entered)

41 032 7

ACH

19. (Cont'd)

Binary digital frequency modulation
Frequency-shift-keying

20. (Cont'd)

using angular feedback demodulation of frequency shift keying (FSK) by means of phase-lock loops.

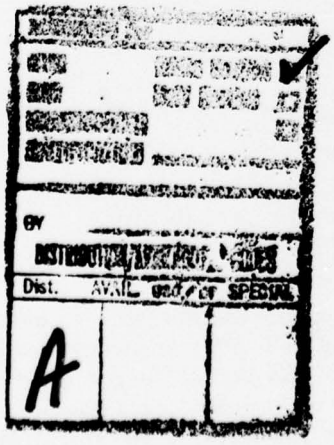

TABLE OF CONTENTS

INTRODUCTION

The objective of this report is to compare probability of error (P_e) vs received signal-to-noise ratio (SNR) for various basic binary, digital, FM transmission schemes. The SNR is the ratio E/η, where E is the energy per bit, and η is the noise power per Hz of bandwidth. The scope of this report is limited to binary rather than multi-level, digital FM for the following reasons:

1. Binary systems are often more practical and economical in terms of design (Ref 1).

2. The available literature for angular feedback FSK (frequency shift keying) demodulators (phase-lock loops) deals primarily with binary systems.

3. Probability of error is more readily analyzed for binary systems.

Figure 1 compares the relative error performance of the systems discussed in this report.

Binary digital FM for rectangular modulating waveforms can be considered as a form of FSK in which the signal wave is treated like an FM signal.

Emphasis will be placed on the phase-incoherent detection schemes because it is generally impractical to maintain a coherent phase reference at the receiver for FSK. In fact, phase shift keyed (psk) transmission offers superior performance and should be used if it is available.

GENERATION OF DIGITAL FM

In generating digital FM signals, phase continuity should be maintained at the switching instants in order to avoid undesirable transients in the FM wave. For this reason, the digital baseband data transitions are fed to an FM modulator rather than switching between different independent oscillators.

The shaped signal at the output of the pre-modulation filter can be described as:

$$S(t) = \sum_{n=-\infty}^{\infty} b_n g(t-nT)$$

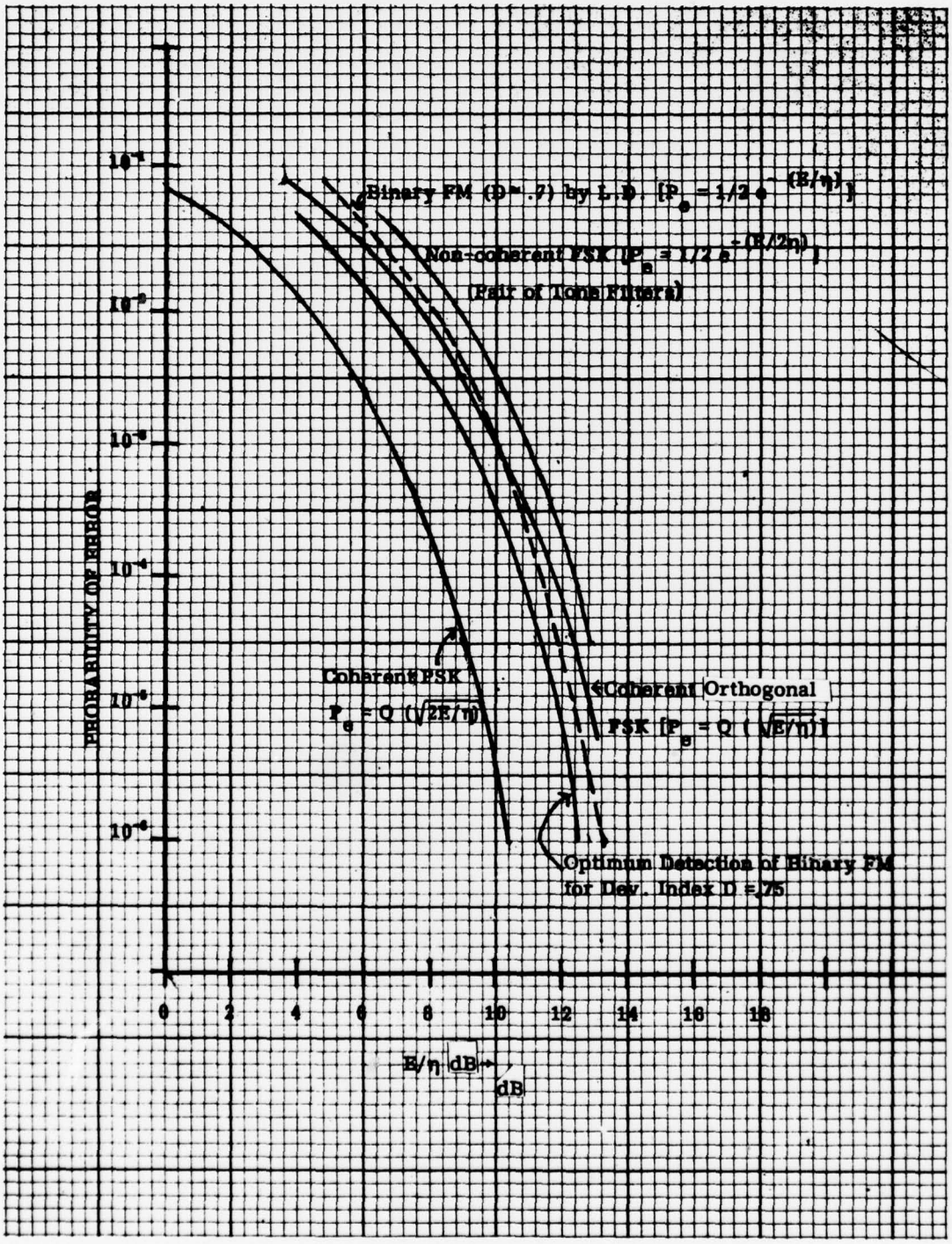

Figure 1 Comparative error rates

Where b_n is the binary data sequence and $g(t-nT)$ represents the filtered pulse which is either positive or negative (corresponding to a mark or a space). The transmitter oscillator frequency follows the baseband (Ref 2).

$$V(t) = A \cos \left[\omega_c t + \theta_o + \mu \int_{t_o}^{t} s(\lambda)\, d\lambda\right]$$

Where A = constant carrier amplitude, ω_c is the carrier frequency, t_o and θ_o are arbitrary reference time and phase, respectively, and μ relates frequency displacement to baseband signal voltage. Another way to visualize the binary FSK process is to consider modulator instantaneous output frequencies constant over the duration of the signal pulses:

$$S(t) = \begin{cases} A \cos 2\pi f_1 t, & \text{For mark} \\ A \cos 2\pi f_2 t, & \text{For space} \end{cases} \qquad 0 < t < T$$

Having generated the digital binary FM signal, the next step is to consider the error rate performance for the various basic detection schemes.

NONCOHERENT DETECTION USING A PAIR OF TONE FILTERS

Noncoherent FSK detection uses only the FM signal envelope amplitude information to decide whether a mark or a space was sent. A pair of tone filters, one centered on the mark frequency and the other centered on the space frequency, is used to detect the binary FM wave as shown in Figure 2 (Ref 3). Since the signal in a filter is a finite bandwidth pulsed sinusoid, there is a partial response, or cross talk, in the other filter. This cross talk is ignored in the following calculation of P_e.

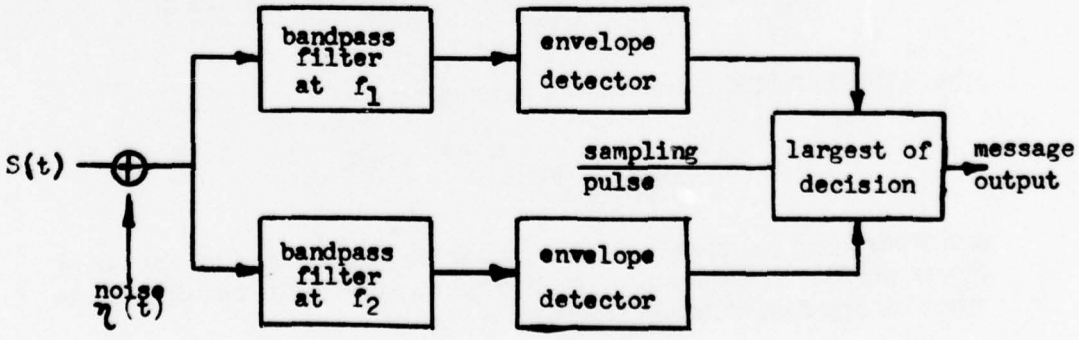

Figure 2 Noncoherent FSK detection

The FSK detector compares the difference of the envelope amplitudes out of the tone filters against a zero threshold which is independent of input SNR. The SNR in the filter output containing the signal is computed in order to obtain an expression for the P_e.

When the instantaneous frequency (mark or space) is the same as the respective filter center frequency, the probability density function (pdf) of the signal in narrow band noise, $P(r_1)$, can be represented in terms of the modified Bessel function of the first kind and zero order (Ref 3):

$$P(r_1) = \frac{r_1}{N} I_o \left[\frac{\mu r_1}{N}\right] e^{-(r_1^2 + \mu^2)/2N} \qquad 0 < r_1 < \infty$$

Where μ = signal level in the filter momentarily containing the signalled tone. The other filter, which contains no frequency component, has a pdf for r_2 of:

$$P(r_2) = \frac{r_2}{N} e^{-(r_2)^2/2N} \qquad 0 < r_2 < \infty$$

An error occurs when $r_2 > r_1$, so that the probability of an error is:

$$P_e = \text{PROB}(r_2 > r_1) = \int_{r_1 = o}^{\infty} P(r_1) \left[\int_{r_2 = r_1}^{\infty} P(r_2) dr_2\right] dr_1$$

This integral relationship reduces to:

$$P_e = 1/2\, e^{-(E/\eta)}\, e^{(E/\eta)/2}\, Q\left(\sqrt{E/\eta}, 0\right) = 1/2\, e^{-(E/\eta)/2}$$

Where the MARCOM Q function is defined by:

$$Q(\alpha, \beta) = \int_{\beta}^{\infty} t\, I_o(\alpha t)\, e^{-(t^2 + \alpha^2)/2}\, dt$$

and where E/η is the ratio of energy per bit, E, divided by the noise power per Hz. This result is plotted together with the results for the other binary demodulation schemes in Figure 1.

OPTIMUM COHERENT FSK DETECTION OF ORTHOGONAL SIGNALS

The optimum, coherent, binary FM detector can be implemented by a pair of matched filters and a sampler which makes a decision on each received bit. Another form of the optimum receiver might use a different matched filter for each of 2N different messages, where N = number of symbols per message. In this case,a single decision will be made as to which message is most likely to have been transmitted.

The optimum receiver receives two transmitted waveforms, corresponding to a mark or a space:

$$S_1(t) = A \cos \omega_1 t$$

$$S_2(t) = \sin \omega_2 t$$

These waveforms satisfy the orthogonality condition:

$$\int_0^T S_1(t) \cdot S_2(t)\,dt = 0, \quad \int_0^T S_1(t) \cdot S_1(t)\,dt = \frac{TA^2}{2}$$

For orthogonality to hold, the frequency separation between S_1 and S_2 must be $w_d = |W_2 - W_1|$, where $w_d T = \eta\pi$, $\eta = 1,2,3,\ldots$. The matched filters can be in the form of integrate-and-dump circuits, one for the mark signal and the other for the space signal. These two matched filters cross-correlate the received signal-plus-noise with the receiver generated replica of either S_1 or S_2. If S_1 is transmitted, the output of the filter matched to S_1 is:

$$V_{f1} = \int_0^T V(t) \cdot S_1(t)\,dt = TA^2/2 + \int_0^T \eta(t) \cdot S_1(t)\,dt$$

The S_2 matched filter output is : $V_{f2} = \int_0^T \eta(t) \cdot S_2(t)\,dt$ The mean of the S_2 filter output is zero, while the variance = η $(T A^2/2)$ for both filters. The optimum receiver decides S_1 (t) was transmitted when the S_1 matched filter output is bigger than the S_2 matched filter output.

The calculation of P_e is facilitated by the signal space representation shown in Figure 3 (Ref 4).

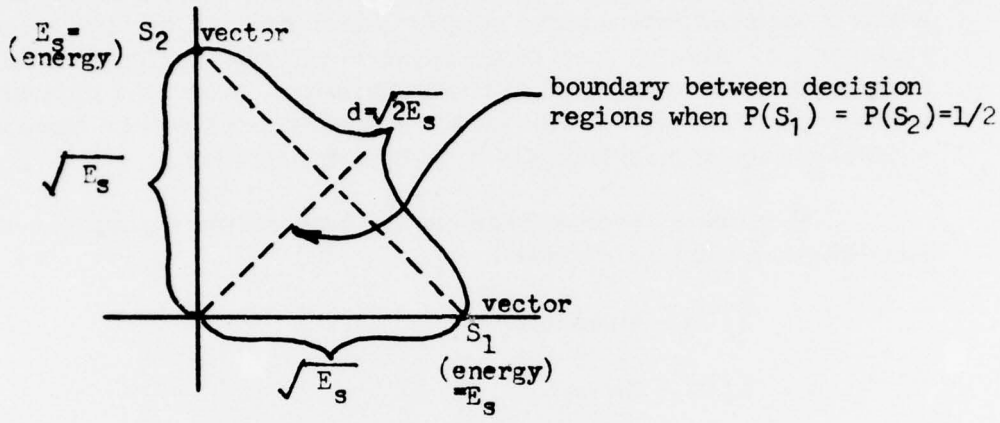

Figure 3 Binary orthogonal signal set

An error occurs when S_1 is transmitted if the noise component exceeds $d/2$, the distance from a signal to a decision boundary. The noise is zero mean gaussian with variance $N_o/2$. Since S_1 and S_2 are assumed to be equally likely, the conditional probability of error is the same, by symmetry, for each signal:

$$P_e = P(S_1)\, P(E/S_1) + P(S_2)\, P(E/S_2) = P(E/S_1)$$

$$\text{and } P(E/S_1) = \int_{d/2}^{\infty} \sqrt{\frac{1}{\pi N_o}}\, e^{-\alpha^2/N_o}\, d\alpha$$

$$= Q\left(\sqrt{\frac{d}{2\,N_o}}\right) = Q\left(\frac{\sqrt{2\,E_s}}{\sqrt{2\,N_o}}\right)$$

$$\text{therefore: } P_e = Q\left(\sqrt{E_s/N_o}\right)$$

This result is plotted in Figure 1 along with the curves for the other digital FM transmission schemes.

PERFORMANCE OF THE LIMITER DISCRIMINATOR

The non-linearity of the FM process and the non-gaussian distribution of post-detection noise makes the prediction of error rates difficult (Ref 5). This difficulty has led to somewhat different models for the transmitter-receiver and different ways of looking at the error mechanism. For example, Salz and others showed that if both transmitting and receiving filters are optimized subject to the constraint that average signal power at the receiver be fixed, the binary error rate performance curve is only about 1/4 dB poorer than the ideal phase modulation with comparison detection (Ref 6). This performance is about 1 dB better than optimally-detected coherent FSK (at $P_e = 10^{-4}$), which signals over the infinite bandwidth white gaussian noise (WGN) channel with an optimum peak-to-peak frequency deviation of 70% of the bit rate. This discrepancy is thought to be due to Salz's inclusion of optimized transmitter and receiver filters which cause the received signal to possess both amplitude and frequency information; the received wave is no longer "pure FM." Another example of the different conclusions that are reached has to do with narrow band FM. Salz and others conclude that, for narrowband FM, clicks make no significant contribution to the error rate (Ref 6). On the other hand, Klapper demonstrates that, for deviation indices greater than 1/2, the major cause of errors is spikes for which the threshold impulse origin encirclement opposes the instantaneous frequency deviation of the signal (Ref 7, 8, 9).

Salz and others analyzed the performance of the limiter discriminator (LD) using a model involving in-phase and quadrature components of the band-limited input signal and an asymptotic approximation of the statistics of the sampled output of the postdetection integrate-and-dump filter (Ref 2, 9, 10). These results show that P_e is affected by system memory and that error curves can be given as bounds for the worst and best data sequences.

Two different analyses of the LD error mechanism are discussed in this report. An analysis by Klapper was selected because his results can be used to explain and predict the observed experimental behavior of angular feedback demodulators (Ref 8, 11). However, the analysis by Shaft yielded theoretical results which agreed more closely with the experimental error-rate performance for the limiter discriminators (Ref 12).

In Shaft's model of the binary FM transmission system, a sequence of data pulses is fed to an FM modulator. The demodulator consists of an LD followed by a sampler and decision network as shown in Figure 4. In order to determine the probability of an incorrect decision, the probability density of the signal (send f_1 or f_2 for "0" or "1", respectively) plus noise is integrated over the region of incorrect decision. At the output of the LD this probability density is Rician (not gaussian). Shaft used the earlier published values for this integration by Meyerhoff and Mazer to determine P_e for a system operating with the following parameters (Ref 12):

1. $b_o T = 1$, where b_o = equivalent noise bandwidth of the IF
   T = bit length

2. $\Delta f = .796/T$ This value for the separation between the two transmitting frequencies (f_1 and f_2) yields the minimum error rate.

The resulting P_e expressed as a function of receiver input bit energy-to-noise density is:

$$P_e = 1/2 \exp(-E/\eta)$$

This result is plotted in Figure 1.

The deviation index is given by $D = T\Delta f$. It turns out that the optimum D = .796, a value very close to the value D = .7, for which the angular feedback demodulator error performance is optimum.

One of the objectives of this report is to outline the advantages of using angular feedback demodulators (which include phase-lock loops). Since the error rate performance of these demodulators is more readily analyzed in terms of threshold impulses (TI) and loss-of-lock impulses (LLI), the Klapper approach will be emphasized. The Klapper approach has the further advantage of predicting P_e when the predetection bandwidth is much wider than the bit rate (due to doppler shifts and system frequency instabilities). There is a link between the threshold mechanism in analog FM and error generation in digital FM in that encirclement spikes are found to be the prime cause of errors, even for carrier-to-noise ratios substantially above the FM threshold level (Ref 11).

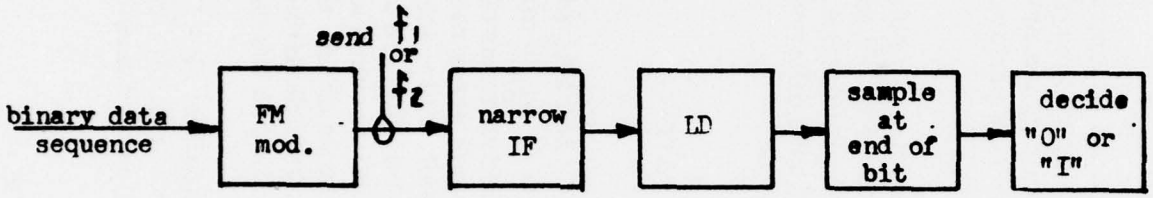

Figure 4 Demodulator, sampler, and decision network

The noise at the output of the LD is composed of a small (Rician) component plus superimposed randomly-occurring threshold impulses. These impulses are generated each time the vector, resulting from the addition of instantaneous noise to the instantaneous signal, encircles the origin.

The encirclement is a 2π jump in phase which, when differentiated, yields a spike of unity area in the frequency vs time plane. These spikes are called threshold impulses. The communication system model used by Klapper (Ref 7) for determining the error rate performance of an LD is shown in Figure 5.

The predetection filter removes out-of-band noise. The integrate-and-dump circuit integrates the LD output for the duration of each bit. The integrator output is proportional to the difference in phase between the beginning and end of each bit. The phase difference due to the signal component having rectangular transitions is:

$$\theta_{SR} = 2\pi \int_0^T \Delta f \, dt = 2\pi \Delta f T$$

The modulation index, D, is defined as $D = 2\Delta f/BR$, where BR = bit rate = $1/T$. In terms of D, the phase difference is $\theta_{SR} = \pi D$. The phase difference introduced by the noise is analyzed in terms of the resultant signal-plus-noise vector. For reasonably small error rates, the noise amplitude for most bit intervals tends to be small and noise does not significantly affect the resultant vector. On relatively rare occasions, the noise is high enough to cause the resultant vector to encircle the origin, giving a 2π phase shift. Since for FSK the carrier is offset, these encirclements usually are in a direction to oppose the signal deviation. Klapper has shown (Fig 6) that errors are made according to the deviation index (Ref 8).

This table is summarized by the equation: $k = D/2$ (using the next higher integer for k), where k spikes occur in bit time interval T. In accordance with Rice's theory, the origin encirclements caused by spikes follow a Poisson distribution:

$$P(k) = e^{-NT} (NT) \, k/k!$$

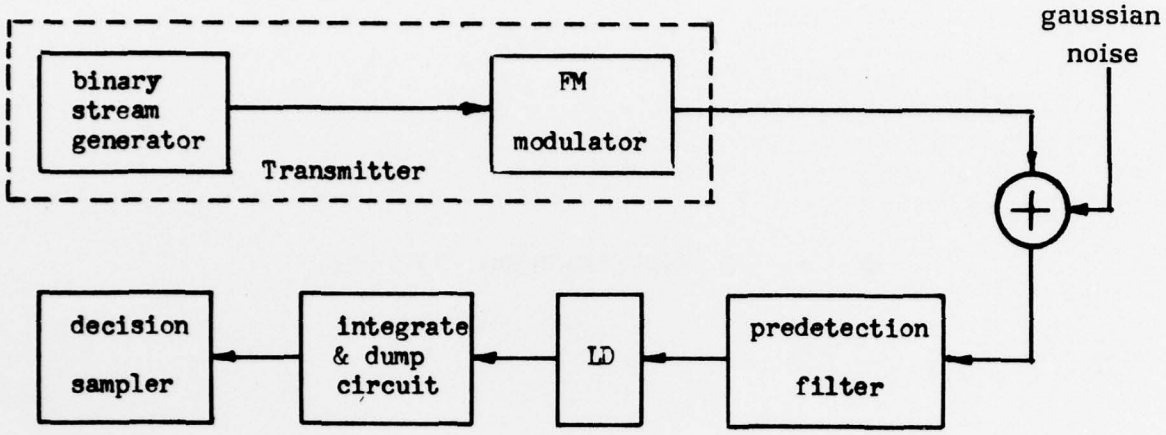

Figure 5 Limiter-discriminator FM system (Klapper)

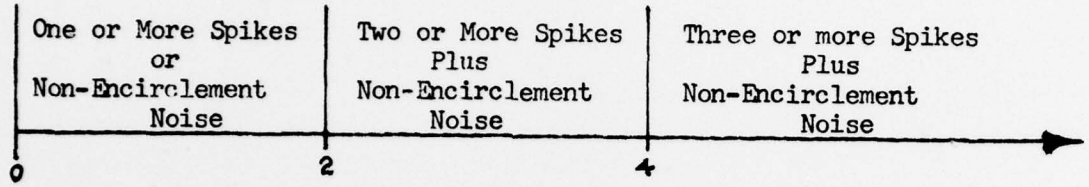

Figure 6 Deviation index, D ------->

where N is the average number of spikes per second. Since the carrier is offset by Δf, the spike rate is approximately (Ref 7):

$$N \approx \Delta f \, e^{-\eta} .$$

Where η = Carrier-to-noise ratio (CNR) at the LD input. The number of spikes per bit is NT. Using the relationship: $D = 2\Delta fT$, $NT = D/2 \, e^{-\rho}$ Then using the Poisson distribution given above, the probability of error is:

$$P_e = \frac{(NT)^k \, e^{-NT}}{k!} \quad , \; k = \text{number of spikes per bit}$$

Figure 7 is a sketch of P_e as a function of the deviation index (D) for a constant noise level, with ρ, the input CNR to the LD, as a parameter (Ref 8). This sketch shows a "zigzag" or staircase behavior.

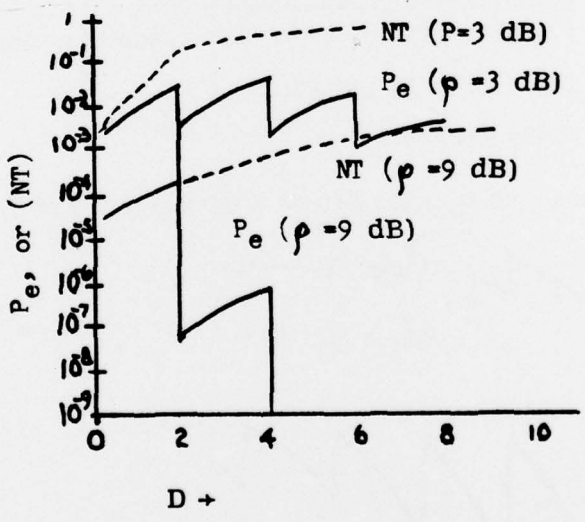

Figure 7 Error probability vs deviation

Experimental error rates obtained for phase-lock demodulators demonstrate the rapid changes in slope or staircase behavior as shown in Figure 7. However, the conventional limiter discriminator shows a smooth monotonic decrease in error rate with increasing CNR. Since the bit energy increases with D, the error rate decreases with D. The smooth curve for the LD is thought to be due to: (1) The smearing of encirclements into adjacent bits caused by narrow predetection filter bandwidth and the effect of other parameters. (2) The presence of nonencirclement (non-impulsive) noise (Ref 7). On the other hand, phase-lock demodulators generally exhibit much greater sharpness of impulses.

In order to compare the LD error curve against the other detection methods, the parameter, ρ, can be expressed in terms of E/η at the receiver input (not at the LD input):

$$E/\eta = K \rho B_N T$$

where: B_n = predetection filter noise bandwidth

ρ = CNR at LD input

T = bit duration

K = unmodualted ρ/modulated ρ
(K is a constant allowing for receiver filter losses)

E = signal energy per bit

η = noise density

Figure 8 is a sketch of P_e vs D, with E/η as a parameter (Ref 6):

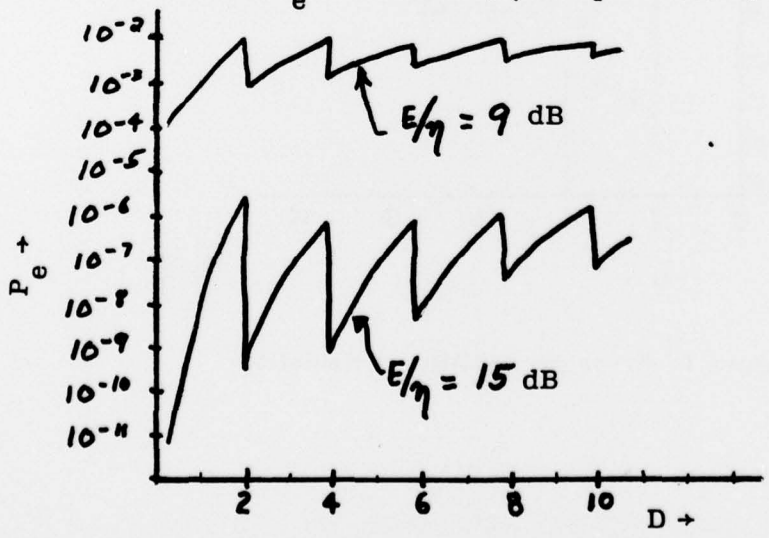

Figure 8 Error probability with E/η as a parameter

PHASE-LOCK LOOP (ANGULAR FEEDBACK) DEMODULATOR

The threshold for analog FM can be significantly reduced by using angular feedback demodulators. Since the error mechanism for analog and digital FM have been shown to be related, there is reason to expect that phase-lock demodulators can also reduce the error rate for digital FM as compared to a LD. In practice, a modified first-order/phase-lock loop (PLL) can give about a ½ dB improvement in error performance (for D = .7 with the predetection on filter bandwidth determined by signal modulation parameters) (Ref 8). This degree of improvement is less than can be achieved for analog FM because: (1) The PLL bandwidth has to be wide enough so that the loop phase error transient response due to frequency steps (FSK data transitions) is within acceptable limits. (2) Ordinarily the receiver predetection filter is relatively narrow since error rate, and not waveform fidelity, is the performance criterion.

The design of PLL for binary FM demodulation is concerned largely with minimization of the total spike rate (TI and LLI). Intersymbol interference is not a problem in practice because as the bandwidth is reduced the PLL starts producing spikes before intersymbol interference becomes unreasonable.

The best type of PLL for demodulation of binary FM is called a modified first-order loop (MFOL) (Ref 11). The MFOL has an active loop filter characterized by a single pole near zero frequency (or at a frequency as low as can be practically achieved) and a zero determined by the loop bandwidth. To achieve a minimum spike rate, the optimum loop bandwidth has been empirically determined to be $B_n = 3.5\,\Delta f$ Hz (Ref 9). As far as the data is concerned, the loop operates as a first-order loop because the asymptotic open loop response has a slope of -6 dB/octave over most of the range (Fig 9). For $D < 2$, the zero gain crossover point of the open loop response is taken equal to the bit rate (Ref 9). This crossover is many times higher than the pole or zero frequency of the active loop filter.

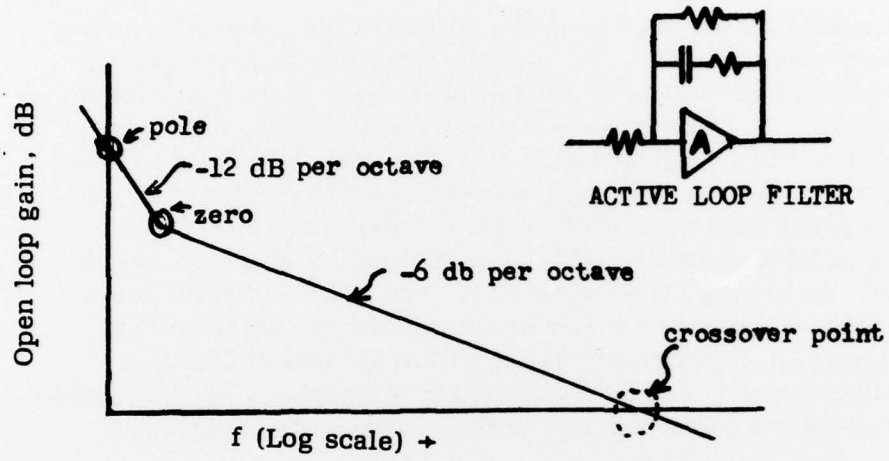

Figure 9 Open loop response

The advantage of the modified first-order loop is that, when the signal input is a series of alternating frequency steps (square wave data), the loop peak phase error is lower than for second-order types (Ref 9). A lower peak phase error is desirable to reduce the frequency of LLI. This transient behavior of a first-order loop for alternating frequency steps is not to be confused with the case where the loop input is a single, non-recurring frequency step, in which case the phase error response is minimum for the critically damped second-order loop.

COMPARISON OF ORTHOGONAL FSK TO PSK

Binary coherent PSK (phase shifts of 90°) is the most efficient signalling scheme. A way to compare coherently detected orthogonal FSK to PSK is to use signal space diagrams. The binary PSK signal vector set is antipodal as shown in Figure 10.

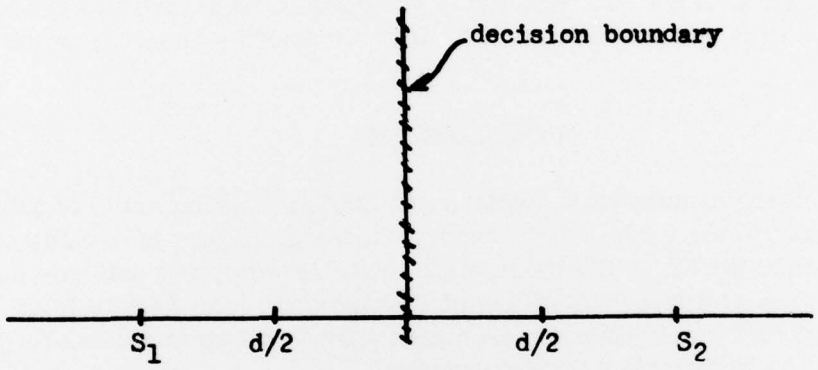

Figure 10 PSK signal set

An error occurs when either vector's distance from the decision boundary (d/2) is exceeded by the zero mean gaussian noise component. The antipodal vector orientation is the "minimum energy" signal set that can be used to communicate at a given error rate. As shown in Figure 3, the distance from a signal vector to the decision boundary is shorter for orthogonal FSK. Hence, the antipodal signalling is 3 dB more efficient than orthogonal signalling. The probability of error for PSK is given by:

$$P_e = Q\ [\sqrt{2E/\eta}\ ]$$

where: E = Signal energy/bit

η = PSD of noise

This result is plotted in Figure 1 along with the Probabilities of Error for the other signalling/detection schemes discussed in this report.

COHERENT DETECTION OF BINARY FM FOR OPTIMUM MODULATION INDEX

The error rate performance for optimum coherent detection of orthogonal signals (using two matched filters) can be bettered by about .85 dB by spacing the tones (θ_1 and θ_2) closer together so that the space filter output is negative when the mark is transmitted and vice-versa (Ref 3). At the optimum deviation index, D = .75 (peak-to-peak frequency deviation, f, is 75% of the bit rate), the mark and space signals are no longer orthogonal, because for orthogonality, $\Delta W\, T = N\pi$, $\eta = 1,2,3,\ldots$. E.F. Smith calculated the probability of error for an optimally detected coherent FSK system operating at D = .75 with the assumption of no interbit dependence in the modulating binary data stream (Ref 13). Smith's result is plotted in Figure 1.

CONCLUSIONS

Conventional telemetry systems are designed using "rule of thumb" or "cookbook" procedures. This report, initiated as part of a study on frequency shift keyed (FSK) modulation, was developed to estimate system improvements attainable by use of a phase-lock loop demodulator. The study of FSK modulation is associated with a transponder locating technique for a munitions recovery system.

It is concluded that the selection of a specific modulation technique, for use in a digital telemetry data link, requires consideration of system parameters. The following factors were considered:

1. Transmission link signal-to-noise ratio
2. Signal bandwidth
3. Data rate
4. Required bit error probability
5. System complexity and cost

It is further concluded that, when FSK-modulated data is demodulated by a phase-lock loop, the required received energy ratio (E/η) can be ½ dB less (for a given error rate) than the conventional limiter discriminator. The particular advantages of this technique were discussed in this report. The various basic binary digital FM systems were compared (Fig 1) for relative error performance.

REFERENCES

1. Sunde, E. D., "Ideal Pulses Transmitted by AM and FM," B.S.T.J., 38, Nov 1959

2. Bennett, W.R., and Salz, J., "Binary Data Transmission by FM Over a Read Channel," B.S.T.J., 42, PP.2387-2426 (1963).

3. Stein and Jones, Modern Communication Principles With Applications to Digital Signalling, McGraw Hill, NY, 1967

4. Wozencraft and Jacobs, Principles of Communication Engineering, John Wiley & Sons, 1965

5. Bennett and Davey, Data Transmission, McGraw Hill, 1965

6. Salz, J., "Performance of Multilevel Narrowband FM Digital Communication Systems," McGraw Hill, NY, 1967

7. Lucky, R.W., Salz, J., Weldon, E.J., Principles of Data Communication, McGraw Hill, 1968

8. Klapper, J., "Demodulator Threshold Performance and Error Rates in Angle-Modulated Digital Signals," RCA Rev 27, Nov 2, 266-244, 1966

9. Klapper, J. and Frankle, J.T., Phase-Locked and Frequency-Feedback Systems, Academic Press, New York, 1972

10. Mazo, J.E. and Salz, J., "Theory of Error Rates for Digiatl FM," B.S.T.J., 45, No. 9, 1511-1535 (1966)

11. Klapper J., Aaronson, G., Acampora, A., Frankle, J., and McLaughlin, P., "Error Rates with Angular Feedback Demodulators," Conf Rec IEEE Telemetering Conf, Houston, Texas, 1968

12. Shaft, P.D., "Error Rate of PCM-FM Using Discriminator Detection," IEEE Trans Set-9, 131-137 (1963)

13. Smith, E.F., "Attainable Error Probabilities in Demodulation of Random Binary PCM/FM Waveforms," IEEE Trans Set-8, No. 4, 290 (1962)

DISTRIBUTION LIST

Commander
USA ARRADCOM
ATTN: DRDAR-LCV
DRDAR-LCP (2)
DRDAR-LCA (2)
DRDAR-LCE
DRDAR-LCS
DRDAR-LCW (2)
DRDAR-LCB (2)
DRDAR-LCF (2)
DRDAR-LCH
DRDAR-LCN (2)
DRDAR-LCU (2)
DRDAR-LCU, M. Margolin (2)
DRDAR-LCU, Dr. L. F. Nichols (2)
DRDAR-LCN-DP, J. Drake
DRDAR-RIA (2)
DRDAR-QA
DRDAR-QAS
DRDAR-QAP
DRDAR-QAN (3)
DRDAR-QAN-T, F. Alfano
DRDAR-QA-QAR (2)
DRDAR-QA-QAT
DRDAR-QA-QAA
DRDAR-QA-FFA
DRDAR-QA-QAM
DRDAR-QA-QAC
DRDAR-QA-QAN-T, G. Frey
DRDAR-TS, COL D. Wright
DRDAR-TS, R. A. Vecchio
DRDAR-TSP
DRDAR-TSI (4)
DRDAR-TSE (2)
DRDAR-TSC
DRDAR-TSB
DRDAR-TSS (5)
DRDAR-TSI-T, W. Donnally (6)
DRDAR-TSI-T, C. Smith
DRDAR-TSI-T, Glass
DRDAR-TSI
DRDAR-TSI-T, W. Barrett

DRDAR-SC
DRDAR-SA
DRDAR-SCP
DRDAR-SCA
DRDAR-SCF
DRDAR-SCW
DRDAR-SCS
DRDAR-SCM
DRDAR-SCN
Dover, NJ 07801

Project Manager
Cannon Artillery Weapon Systems
ATTN: DRCPM-CAWS (2)
Dover, NJ 07801

Project Manager
Selected Ammunition
ATTN: DRCPM-SA (2)
Dover, NJ 07801

Project Manger
Army Gun Defense System
ATTN: DRCPM-ARGADS (2)
Dover, NJ 07801

Project Manager
Munitions Production Base Modernization
ATTN: DRCPM-PBM
Dover, NJ 07801

Commander/Director
Chemical Systems Laboratory
USA ARRADCOM
ATTN: DRDAR-CL
Aberdeen Proving Ground, MD 21010

Director
Ballistic Research Laboratory
USA ARRADCOM
ATTN: DRDAR-BL
DRDAR-BL, W. H. Mermagen
DRDAR-BL-BLP (2)
DRDAR-BL-BLB (3)
DRDAR-BL-BLL (2)
Aberdeen Proving Ground, MD 21005

Defense Documentation Center
Cameron Station
Alexandria, VA 22314 (12)

Commander
Naval Ordnance Laboratory
ATTN: Library
Silver Spring, MD 20910

Director Research & Development
Department of the Air Force
ATTN: Technical Library
Washington, DC 20330

Hdqtrs, Air Force Armament Laboratory (ATX)
Eglin Air Force Base
Florida 32542

US Army Yuma Proving Ground
ATTN; Library (STEYP-AD) (3)
Yuma, AZ 85364

Commander
Wright-Patterson AFB
ATTN: Library (2)
Dayton, OH 45433

Hdqtrs, Air Force Systems Command (SCTS)
Andrews Air Force Base
Maryland 20331

Hdqtrs, Air Force Weapons Laboratory (WLX)
Kirtland Air Force Base
New Mexico 87117

Commander
Air Research & Development Command
ATTN: Technical Library
Baltimore, MD 20101

Redstone Scientific Information Center
US Army Missile Research and
Development Command
ATTN: Chief, Document Section
Redstone Arsenal, AL 35808

Commander
Harry Diamond Laboratories
ATTN: Library, Bldg 92 (3)
AMXDO-RB/530, Mr. T. Liss (2)
Washington. DC 20438

Naval Ammunition Depot
ATTN: Library (2)
Crane, IN 47522

Army Material & Mechanics Research Center
ATTN: Library (2)
Watertown, MA 02172

Director
Lawrence Radiation Laboratory
ATTN: Library
P.O. Box 808
Livermore, CA 94550

Sandia Corporation
ATTN: ORG 7282, Mr. Bentz
ORG 7262, Mr. R. Bentley
ORG 7284, Mr. D. Williams
Library (3)
P.O. Box 5800
Albuquerque, NM 87115

US Naval Weapons Center
ATTN: Technical Library (2)
China Lake, CA 93555

Chairman. Telemetry Group
ATTN: Mr. G. E. Wooden
BMDSC-RD
P.O. Box 1500
Huntsville, Alabama 35807

Commander
White Sands Missile Range
ATTN: Technical Library
White Sands, NM 88002

Physical Science Laboratory (PSL)
New Mexico State University
MRS/WSMR
ATTN: Lloyd Griffin
P.O. Box PSL
Las Cruces, NM 88003

US Test & Evaluation Command
ATTN: DRSTE-SG-H
Aberdeen, MD 21005